ENCIT2024
20th Brazilian Congress of Thermal Sciences and Engineering

ABCM Associação Brasileira de Engenharia e Ciências Mecânicas

20th Brazilian Congress of Thermal Sciences and Engineering
November 10th-14th, 2024, Foz do Iguaçu – PR - Brazil

ENCIT2024-0061
NUMERICAL HEAT TRANSFER EVALUATION OF ABSORBER FOAMS WITH APPLICATION IN VOLUMETRIC RECEIVERS

Carlos de Jesus Silva de Oliveira
d2024007762@unifei.edu.br
Kelvin Johnson Oliveira
kelvinjohnson1028@gmail.com
Victor Tertuliano Macedo
tertu.victor123@gmail.com
Lucas Giarola Chinellato
lucaschinel@gmail.com
Paulo Mohallem Guimarães
pauloguimaraes@unifei.edu.br
Rogério Fernandes Brito
pauloguimaraes@unifei.edu.br
Ricardo Luiz Perez Teixeira
ricardo.luiz@unifei.edu.br
Carlos Henrique de Oliveira
carloshenrique.unifei@gmail.com
Federal University of Itajubá - Itabira Campus
Rua Irmã Ivone Drumond, 200, Distrito Industrial II, Itabira, Zip.: 35903-087, MG, Brazil

Carlos Henrique Alexandrino
carlos.alexandrino@ufvjm.edu.br
Federal University of Vales do Jequitinhonha e Mucuri
Rua da Glória, 187, Centro, Diamantina, ZIP.: 39100-000, MG, Brazil

Abstract. *This is a numerical heat transfer study in foams with application in volumetric receivers applied in solar plants based on concentrating solar radiation. Solar radiation coming from heliostat field is concentrated in receivers at the top of a tower. The receiver consists of some enclosures named secondary concentrator, a window glass dome, an absorber media and an external pressurized vessel. The secondary concentrator focuses solar radiation into the glass window. The radiation goes through the glass window to the absorber porous media located inside the pressurized receiver. Absorber porous matrix transfers heat to a heat transfer working fluid. In this work, this heat transfer agent is pressurized air. Colder pressurized air enters the volumetric receiver confined inlet and exits through an outlet under higher temperatures. Then the hot air is used in some thermodynamic cycles to produce electricity. A numerical simulation package (COMSOL MULTIPHYSICS ®) is used in order to approximate solutions as an attempt to improve thermal efficiency of the receiver by considering convection and conduction heat transfer in laminar and turbulent regime inside a volumetric receiver through a porous structure that has a certain porosity and thickness. Heat flux is prescribed as a mean of radiation energy source. The mathematical model and the numerical techniques are validated with some benchmark problems found in literature. It is known that porosity may enhance heat transfer by working as an absorber media. However, the porous media may induce a pressure drop that may interfere in the whole process. Some materials are studied as porous absorber media: ceramic, alumina, silicon carbide and graphene. It is observed that the porous media strongly plays its role to increase the contact area of air to be heated and the solid conductive material*

Keywords*: Concentrating Solar Plant, Volumetric Receiver, Heat transfer, Solar Power Tower, Turbulence*

1. INTRODUCTION

Clean and renewable energy generation is among the most discussed topics by the scientific community, due to the drawbacks of traditional source (fossil fuel) and the world energy consumption increase. The large-scale application of clean, low-carbon renewable energies has become a global consensus to resolve pressing issues such as climate change, environmental pollution, and energy shortage. Concentrated solar power (CSP) is a clean generation that has gained major focus of research over the last fifty years. Among various types of renewable energies, solar energy has a bright prospect due to its vast amount, clean utilization and easy access. In order to overcome the major problems associated with solar

energy harvesting such as low energy density and inefficient energy conversion, concentrating solar power (CSP) technology has become one of important methods to convert solar energy to electricity.

The main source of CSP is the more abundant energy in the environment, the sun. There are four technology types: Parabolic, Dish, Central Tower and Fresnel. Central tower power plants with volumetric concentrator have shown high performance in the production of clean and cheap energy.

A study by Behar (2013) analyzed researches related to solar thermal power plants with central receiver, indicating that systems with volumetric receiver technology have great energy potential. In turn, Avila-Martin (2011) reviewed types of volumetric receivers, indicating the receiver from REFOS program as the most efficient. Albanakis (2009) studied types of porous materials which have better performances in thermal energy convection to the system fluid.

The study of Buck (2001) demonstrated that plants using volumetric central receiver has the potential to compete in today's market. In 2031, one system with central volumetric receiver was built by Del Río. Currently, It is on the first test phase using part of the solar field of Solugas. Later, this innovation will be applied to the Abengoa plant, allowing its entry into the market and reducing the cost of energy.

Based on the Generation 3 Concentrating Solar Power Systems (CSP Gen3) presentation roadmap, the system operating temperature should be further raised to above 700 ºC in order to achieve the aimed 50% solar-to-electricity conversion efficiency (Mehos et al., 2017; He et al., 2020). Nonetheless, there are still many demands in solar receiver designs, high temperature material level, energy storage subsystem optimization. In CSP systems, the solar receivers are directly irradiated by solar radiation and their safe and high-efficiency performance is the main reason, not only to increase the overall solar-to-electricity conversion efficiency, but also to reduce the Levelized Cost of Energy (LCOE) (Li and Tao, 2017, Dowling et al. 2017). Taking into consideration the solar absorption mechanism, solar receiver systems could be mostly separated into three categories: tubular receiver, volumetric receiver, and particle receiver. The volumetric solar receiver distributes the incoming solar radiation into a three-dimensional space. The concentration of solar flux on the receiver surface is reduced and the maximum allowable solar flux on the aperture of the receiver is increased. In general, the volumetric absorption of solar radiation could be implemented by both the heat transfer fluid and porous media. Porous materials are widely used for solar absorption due to their large porosity and interconnected porous matrix.

The common porous structures include honeycombs, wire meshes, packed beds, and foams made from metallic or ceramic materials. The concentrated solar radiation infiltrates the porous structure and is gradually absorbed. The heat transfer fluid (normally air) passes through the porous structure and exchanges heat with the high temperature porous media. In a more convenient case, the fluid and porous medium temperature increases gradually along the main flow direction featuring the known phenomena named volumetric effect (Kribus et al., 2014, A and B). Porous volumetric solar receivers show efficiency for increasing the solar-to-thermal conversion. However, there are some heat transfer drawbacks such as strong coupling, multiscale, and multimode pose challenges in experimental and numerical analyses. For that being so, a number of parameters such as geometries, optical and thermophysical properties of the porous media as well as the incident solar radiation distribution may influence the fluid flow and heat transfer processes in porous volumetric solar receivers. Moreover, the small scale of porous channels and the large scale of CSP systems require multiscale modeling of fluid flow and heat transfer, in the porous volumetric solar receiver. Finally, multiple heat transfer mechanisms such as solar radiation transfer, heat conduction in the porous media, convective heat transfer between the porous matrix and the heat transfer fluid, and radiative heat transfer create difficulties in evaluating the performances of the porous volumetric solar receiver. Eventually, many studies have been carried out on heat transfer in porous volumetric solar receivers creating new methods for enhancing volumetric receiver efficiency in Concentrating Solar Power Plants.

In the present work, it is performed a numerical heat transfer study using metallic foams with application in volumetric receivers applied in solar plants. The working fluid is pressurized air. A numerical simulation package (COMSOL MULTIPHYSICS ®) is used in order to approximate solutions as an attempt to improve thermal efficiency of the receiver by considering convection and conduction heat transfer in laminar and turbulent (k-ω) regimes inside a volumetric receiver through a porous structure that has a certain porosity and thickness. Heat flux is prescribed on the absorber surface as a mean of considering the solar irradiation source. The mathematical model and the numerical techniques are validated with a benchmark problem found in literature. Also, the laminar and turbulent models are considered to take into consideration the high pressurized air at the entrance of the volumetric receiver. It is known that porosity may enhance heat transfer by working as an absorber media. However, the porous media may induce a pressure drop that may interfere in the whole process that may bring structure damage. Some materials are studied as porous absorber media: Alumina, silicon carbide. It is observed that the porous media strongly plays its role to increase the contact area of air to be heated and the solid conductive material.

2. RECEIVER DESIGN AND PROBLEM FORMULATION

The problem consists of a volumetric receiver, considering steady laminar and turbulent forced convection. This first analysis takes into consideration air as the working fluid and Silicon Carbide and Alumina as the solid materials in the porous media matrix. Figure 1 depicts the geometry and the boundary conditions of the problem. The computational domain consists of four subdomains that are signalized by the squares in Fig. 1. These subdomains are the air domain (regions 1, 2 and 3) and the porous media domain (region 4). Table 1 shows the properties of Silicon Carbide, Alumina

and air, respectively. The boundary conditions are shown by the circles which are related to the surfaces the circles are in contact with.

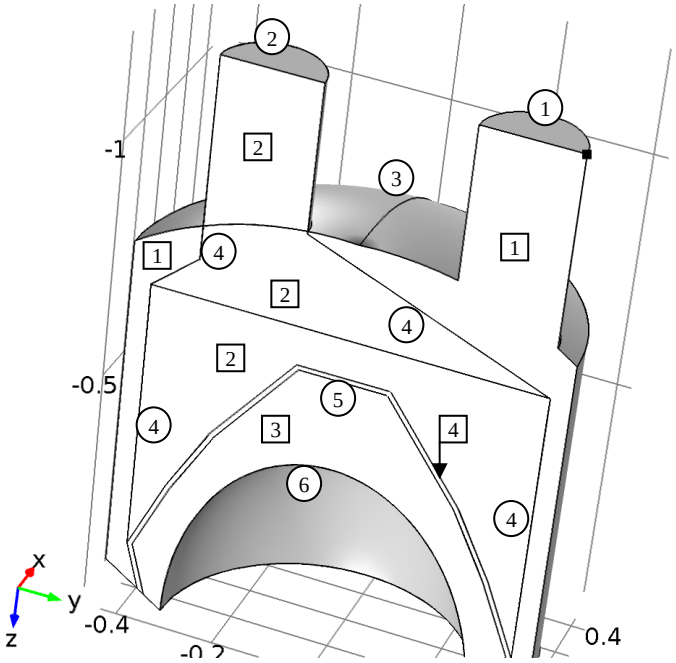

Figure 1 – Geometry and boundary conditions.

For Silicon Carbide:
Surface 1 : inlet: Pressurized air velocity (V_0): 0.5m/s, temperature (T_0): 293.15 K;
Surface 2: outlet: developed flow conditions;
Surface 3, 4, 6: outer walls: no-slip condition, thermal isolation;
Surface 5: Temperature: 800K;
For Alumina:
Surface 1 : inlet: Pressurized air velocity (V_0): 0.01m/s, temperature (T_0): 293.15 K;
Surface 2: outlet: developed flow conditions;
Surface 3, 4, 6: outer walls: no-slip condition, thermal isolation;
Surface 5: Heat Flux: 100W/m/^{2};
All surfaces belonging to the cut plane are under symmetry conditions (flow and heat symmetry).

Table 1. Properties of Silicon Carbide and Alumina.

Name	**Value**	**Unit**
Silicon Carbide		
Heat capacity at constant pressure	900[J/(kg*K)]	J/(kg*K)
Density	3100[kg/m^3]	kg/m^3
Thermal conductivity	150[W/(m*K)]	W/(m*K)
Permeability	0.0001	m^2
Ratio of specific heats	1	1
Dynamic viscosity	1	Pa*s
Young's modulus	300e9	[Pa]
Poisson's ratio	0.14	

Alumina		
Heat capacity at constant pressure	900	[J/(kg*K)]
Density	3900	[kg/m^3]
Thermal conductivity	27	[W/(m*K)]
Permeability	0.5	[m^2]
Ratio of specific heats	1	1
Dynamic viscosity	1	Pa*s
Young's modulus	300e9	[Pa]
Poisson's ratio	0.222	

On the surfaces interfacing two different domains, appropriate boundary conditions are imposed in relation to one another. The basic governing equations (without the turbulence treatment) for such a problem are:

1) For the fluid domain:

The mass conservation equation:

$$\nabla.(\rho\mathbf{u})=0 \tag{1}$$

The momentum conservation equation:

$$\rho(\boldsymbol{u}.\nabla)\boldsymbol{u}=\nabla.\left[-p\boldsymbol{I}+\mu(\nabla\boldsymbol{u})+(\nabla\boldsymbol{u})^{T}-\frac{2}{3}\mu(\nabla\boldsymbol{u})\boldsymbol{I}\right] \tag{2}$$

The energy conservation equation:

$$\rho C_p\boldsymbol{u}\nabla T=\nabla.(k\nabla T) \tag{3}$$

where $\boldsymbol{u}$ is the fluid velocity vector, ρ is the fluid density, $\boldsymbol{I}$ is the identity vector, μ is the dynamic viscosity, *Cp* is the specific heat, *k* is the fluid thermal conductivity, *p* is the pressure and *T* the is the temperature.

2) For the porous matrix (Brinkman's equations)

$$\frac{\rho}{\varepsilon_p}\left((\boldsymbol{u}.\nabla)\frac{\boldsymbol{u}}{\varepsilon_p}\right)=\nabla.\left[-p\boldsymbol{I}+\frac{\mu}{\varepsilon_p}\left(\nabla\boldsymbol{u}+(\nabla\boldsymbol{u})^{T}\right)-\frac{2\mu}{3\varepsilon_p}(\nabla.\boldsymbol{u})\boldsymbol{I}\right]-\left(\mu K^{-1}+\beta_F|\boldsymbol{u}|+\frac{Q_{br}}{\varepsilon_p^2}\right)\boldsymbol{u} \tag{4}$$

$$\rho\nabla.\boldsymbol{u}=Q_{br} \tag{5}$$

where ε_p is porosity and *K* is the permeability.

3) Heat transfer in porous media

$$\rho C_p\boldsymbol{u}\nabla T=\nabla.(k_{eq}\nabla T) \tag{6}$$

$$k_{eq}=\theta_p k_p+(1-\theta_p)k \tag{7}$$

where θ_p is the volume fraction, k_p is the effective thermal conductivity fluid of the fluid-solid mixture.

3. VALIDATION

One of the validations was the porous media problem whose results were contrasted with the ones by Hossain and Wilson (2002). It is a study of natural convection in a square cavity containing porous medium. T_c is the temperature on the cold surfaces and T_h is the temperature on the heated surfaces. There is a region on the bottom right vertical wall where the temperature varies linearly. This validation can be found in Comsol Multiphysics ® documentation. Temperature and velocities behaviors are contrasted. There is an excellent agreement.

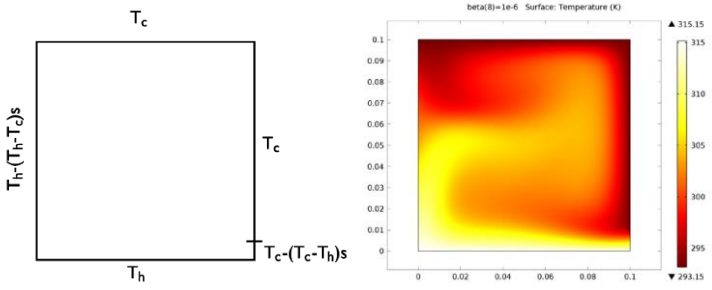

Figure 2 – Geometry, boundary conditions and the isotherms for Rayleigh number equal to 10^5.

4. NUMERICAL METHOD

The Comsol Multiphysics was used to approximate solutions to the governing equations. The finite element method is used. Figure 3 shows the meshes and Table 2 shows the mesh statistics for the two cases.

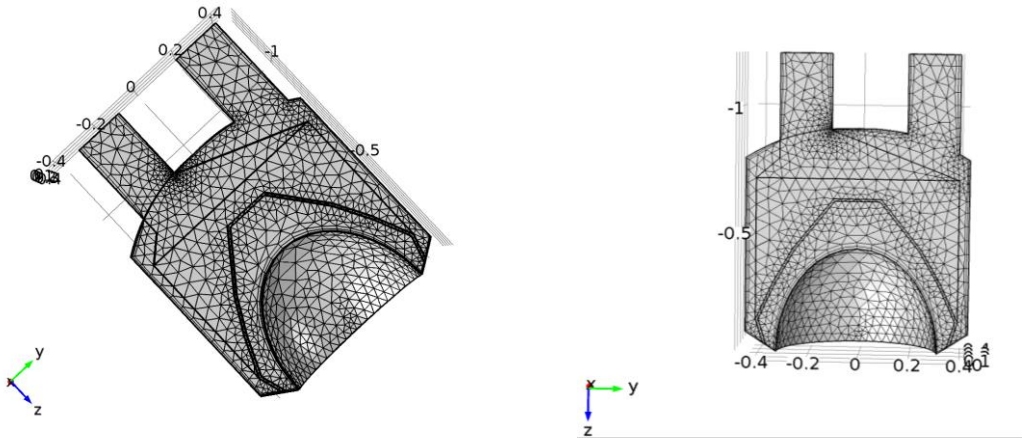

a) Laminar regime b) Turbulent regime

Figure 3 – Mesh with tetrahedrical elements.

Table 2. Mesh statistics.

Property	Value
Laminar Regime – Silicon Carbide	
Minimum element quality	0.007453
Average element quality	0.5319
Tetrahedral elements	46403
Pyramid elements	1012
Prism elements	10496
Triangular elements	9810
Quadrilateral elements	428
Edge elements	975
Vertex elements	61

Property	Value
Turbulent Regime - Alumina	
Minimum element quality	0.005496
Average element quality	0.5349
Tetrahedral elements	46360
Pyramid elements	1012
Prism elements	10496
Triangular elements	9788
Quadrilateral elements	428
Edge elements	975
Vertex elements	61

5. RESULTS

5.1 Results for laminar regime

Figure 4 shows the thermal field of the four domains: a) entrance zone where air enters the system and goes until it reaches the porous media, b) exit zone which is the domain after leaving the porous media , c) intermediate zone which is the domain between the glass dome and the porous media and d) the porous matrix. The entrance region (a) temperature varies from 293 to 800k. This more heated region is placed on the lower region that is in contact with the porous region surface that is at 800 K. Air is significantly heated as it passes through the porous region. In the exit region (b), that is the region after the porous matrix, temperature ranges from 621K to 796K. It is worth seeing that the coldest place in this region is in its lower part. There was about a 273% temperature increase when comparing to the inlet air temperature of 293.15K. This is due to the porous medium effect that plays a role of augmenting the thermal contact between air and the porous material. Region (c) presents almost a uniform temperature of 800K. The thickness of this porous layer is small and the solid material used with moderate thermal conductivity (k = 27 W/m.K). An interesting study here is to optimize the thickness of this porous matrix in order to achieve the best heat transfer possible taking into consideration pressure load gained and material cost.

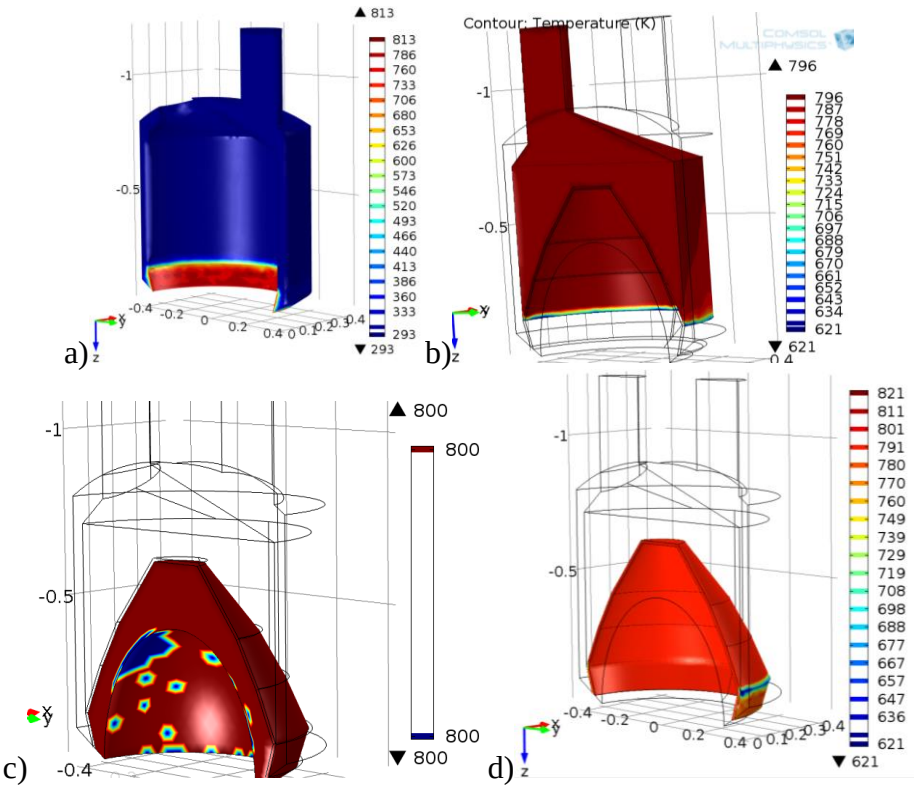

Figure 4 - Isotherms for the four domains (V_0 = 0.5 m/s, T_0 = 293.15K, T_{matrix} = 800K and p_0 = 15 bar)

Figure 5 shows the streamlines for the case from Fig. 4. For a velocoity entrance of 0.5 m/s, the flow field seems to be organized with no significative recirculations. One can observe the air passing thorugh the porous media. This geometry assures that the air (red lines) moves from the entrance tube and then flows over the internal chamber and then reaches the lower porous media inlet. It seems to be interesting to analyse the velocity field to check if air flow is uniform on the porous media inlet.

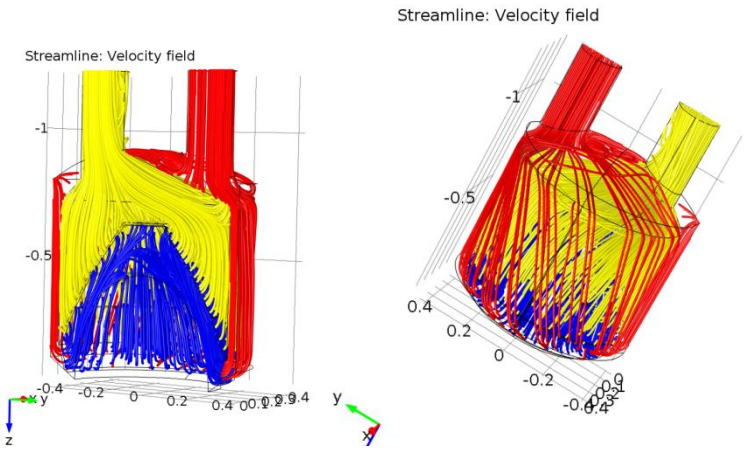

Figure 5 - Streamlines (V_0 = 0.5 m/s, T_0 = 293.15K, T_{matrix} = 800K and, p_0 = 15 bar)

Figure 6 presents the velocity field for the four domains for the case from figure 4. For the porosity of 0.4, the exit velocity is almost four times bigger than the entrance velocity, although the tubes have the same diameter. It is interesting to analyse in future works the air compressibility for this kind of systems. In this test case, air is considered incompressible. As expected, the velocities in the porous media are lower. Due to the incompressibility effect, higher velocity regions have lower pressure fields (see Figure 7). One point that must be taken into consideration for future studies is the high pressure difference in the porous matrix. Silicone Carbide is being used in the porous matrix as due to it supports great pressure differences, thermal shock and water hammers caused by turning on and off of turbines in the net.

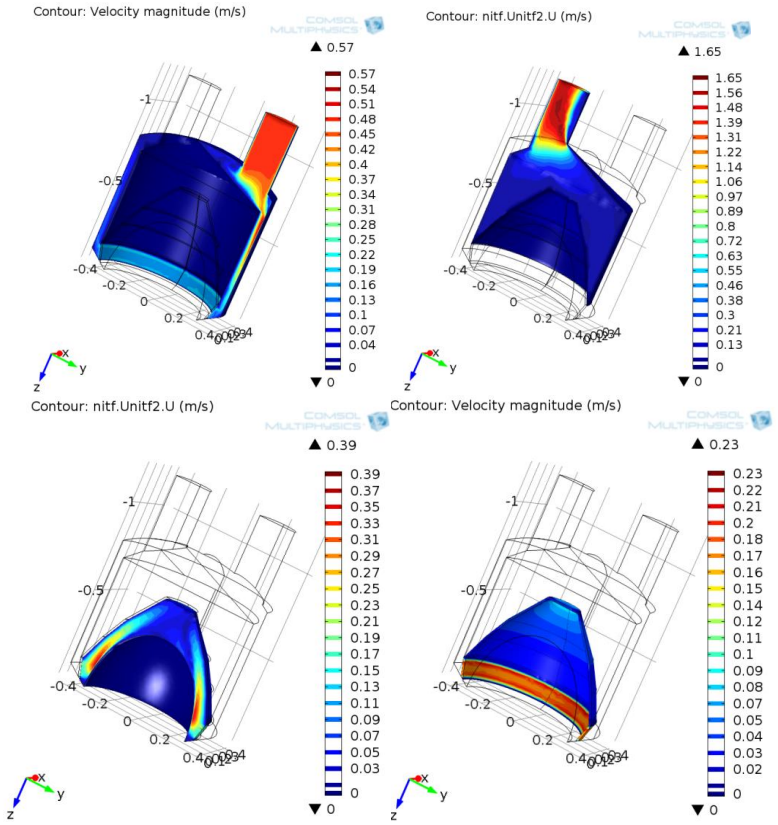

Figure 6 - Velocity field (V_0 = 0.5 m/s, T_0 = 293.15K, T_{matrix} = 800K and p_0 = 15 bar)

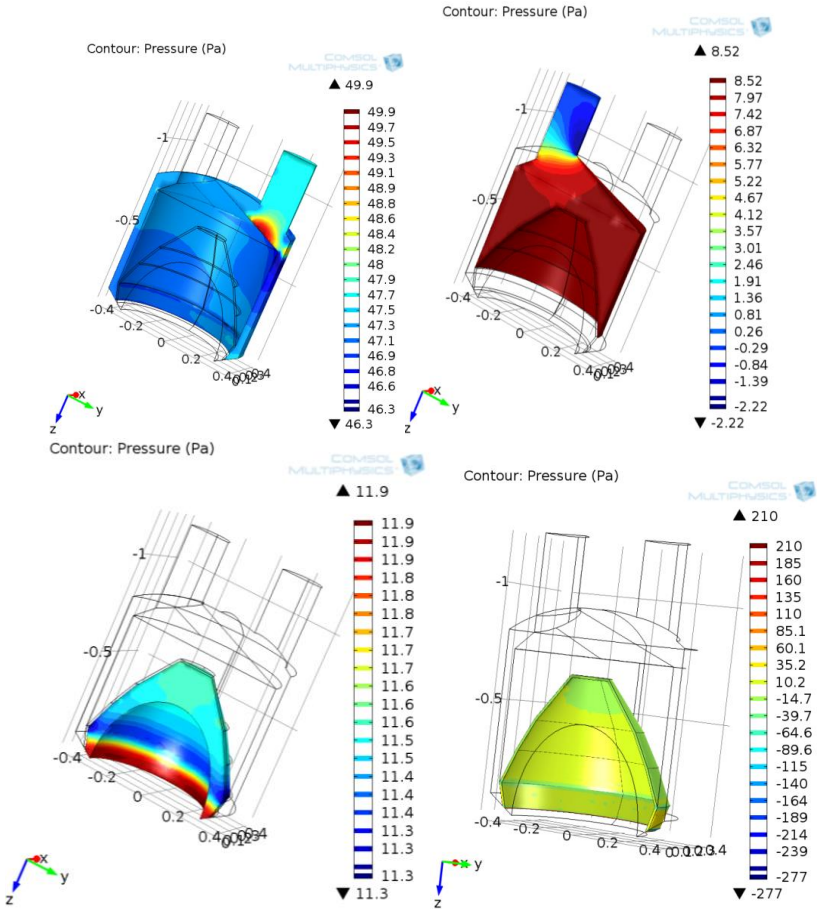

Figure 7 - Pressure field (V_0 = 0.5 m/s, T_0 = 293.15K, T_{matrix} = 800K and p_0 = 15 bar)

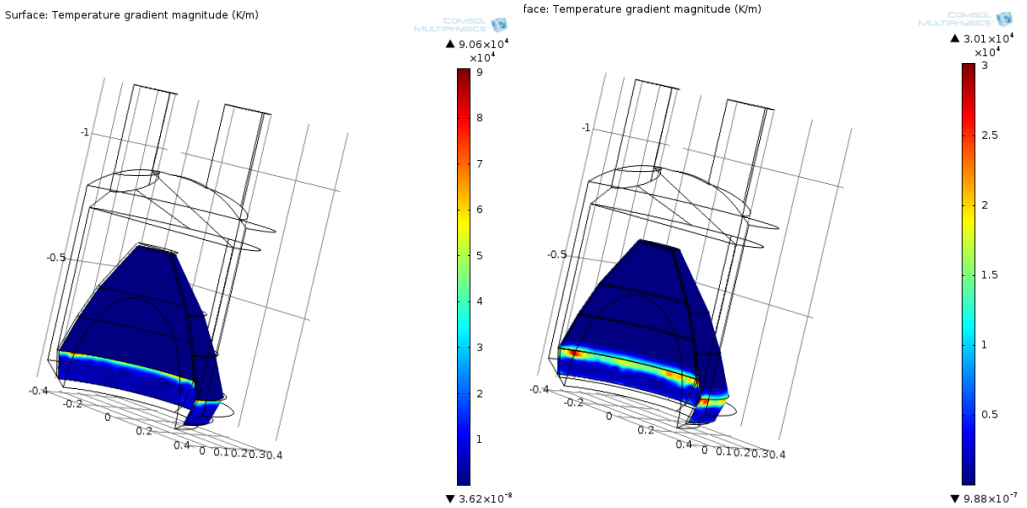

a) Inner surface of the porous media b) Outer surface of the porous media

Figure 8 - Temperature gradients of the inner and outer surfaces of the porous media (V_0 = 0.5 m/s, T_0 = 293.15K, T_{matrix} = 800K and p_0 = 15 bar)

In Fig. 8, one can see the behavior of the temperature gradients of the porous material on its inner and outer surfaces. Just in accordance with the temperature field, there are greater gradients near the upper part of the lower entrance region. Figure 9 also depicts the gradient temperatures inside the porous media.

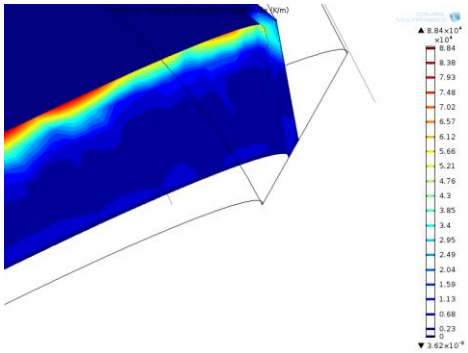

Figure 9 - Temperature gradients of the porous media (V_0 = 0.5 m/s, T_0 = 293.15K, T_{matrix} = 800K and p_0 = 15 bar)

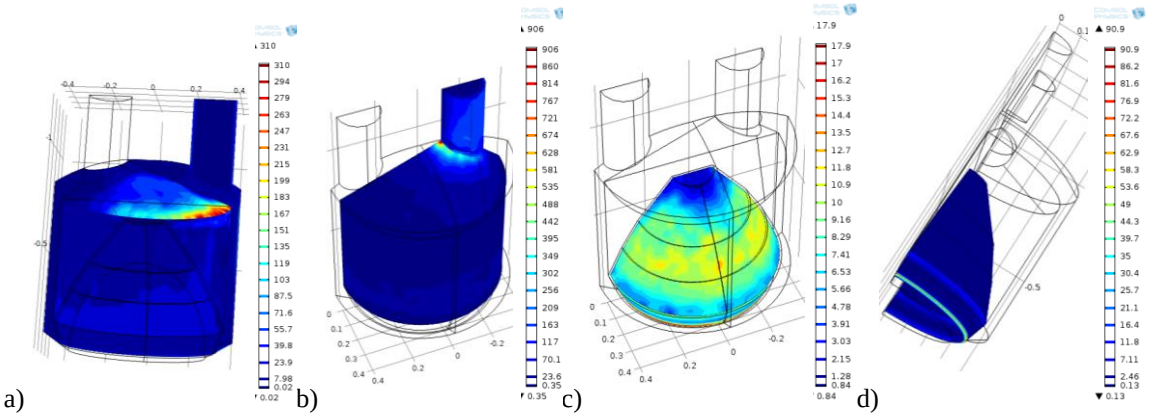

a) b) c) d)

Figure 10 - Shear rate behavior.

Figure 10 shows the shear rate in the entrance domain (a), the exit domain (b), the intermediate domain (c) and the porous matrix domain. Shear rate is the rate at which a progressive shearing deformation is applied to some material or to the walls. As expected, borders are likely to have higher shear stresses. One may note that in the shear stress is not related to the field with highest pressure. For instance, the domain with highest average shear stress is the exit domain whereas the region that presents the highest average pressure field is the porous media. However, the field that shows the highest is the one with higher average temperatures.

Finally, Figure 11 depicts the conductive and convective heat fluxes in the porous media. Heat convection is clearly higher in the bottom of the matrix. When the fluid passes through the bottom, this region is already heated and then the fluid passes through the porous matrix again, to find its path to the exit region.

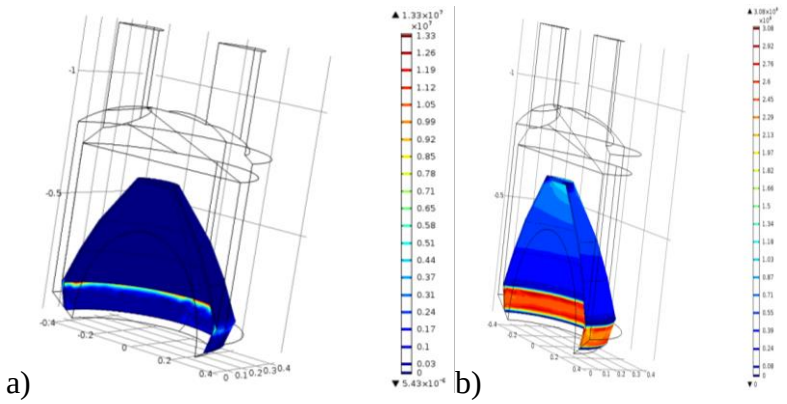

a) b)

Figure 11 - Conductive (a) and convective (b) heat fluxes in the porous media.

5.2 Results for turbulent regime

Figures 12 to 15 consider turbulence models for Alumina and permeability of 0.5m^2. Also, the entrance uniform velocity is 0.01m/s.

One can see in Figure 12 that for the boundary conditions used, the streamlines do not show a flow featuring a turbulent regime with vortices. This is due, for a first analysis, the entrance velocity (0.01m/s) and heat flux (100W/m^2) which may induce laminar features. When implementing a turbulent model, many attempts were carried out to reach solution. That is why smooth boundary conditions were here. In a future work, a sweep analysis is going to be used to reach higher entrance velocities and more real heat fluxes.

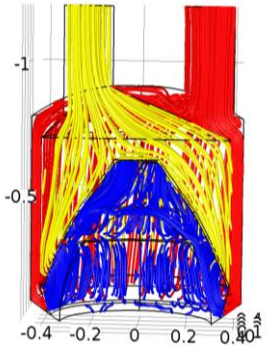

Figure 12 – Streamlines for the three domains.

Figure 12 depicts the temperature field. The maximum temperature is 361 K in this domain and it happens in the exit to the porous media where heat flux is applied. It is important to mention that the inner walls are considered adiabatic and is why the cold air entering the system is not heated. This situation is different from what happens in the real problem. A more appropriate boundary condition must be applied at such walls such as similar temperature as the inner heated air near the inner wall. This is material for future approach. The maximum temperature is quite below the maximum temperature found for the laminar case due to the materials are different and also in the laminar case, it was specified temperature of 800K in the absorber surface. In addition to this, the entrance velocity is 0.01m/s compared to 0.5m/s for the laminar case.

Figure 13 shows the temperature field for the porous matrix. A maximum value of 532K is achieved which is much lower than for the laminar case due to the reasons already mentioned before. It is interesting to observe how the temperature rises as one move to the center of the matrix. This is in consonance with the temperature in Fig. 14. When comparing the behavior in Fig. 14 (heat flux imposed in the absorber surface) with Fig. 4 (temperature imposed in the absorber surface), in the same porous domain, the case with uniform temperature on the absorber surface shows quite a uniform temperature in the whole matrix. While for the heat flux boundary condition, the temperature field gradually rises from 350K to 532K. It seems there is a higher temperature gradient when heat fluxes are imposed. The temperature values for the temperature imposed are higher, though.

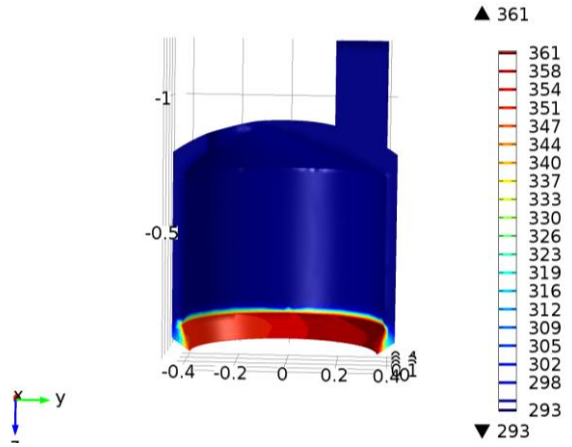

Figura 13 – Temperature field for the entrance domain.

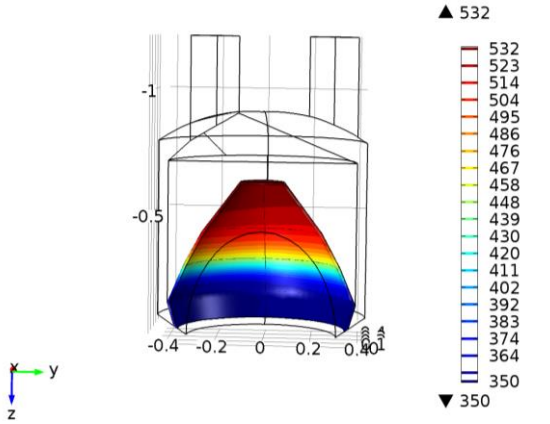

Figure 14 – Temperature field in the porous matrix.

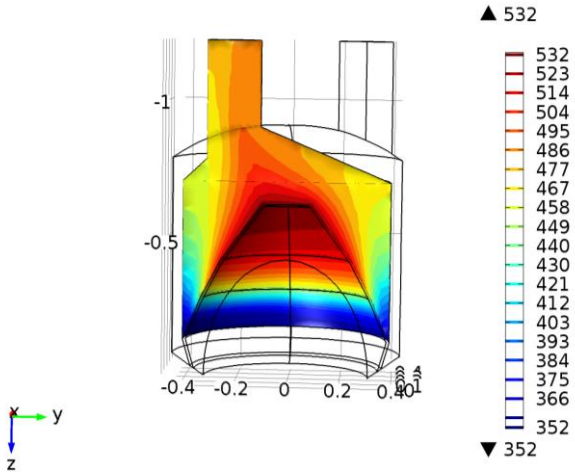

Figure 15 – Temperature field in the exit domain after the porous matrix domain.

Figure 15 shows the temperature field of air exiting the porous media and flow through the exit domain. Some similar features are found here as in Figure 14 when it comes to the temperature gradient. Also, the temperature becomes higher when approaching the core of this domain. It seems that the thermal behavior for heat flux as boundary condition is in more agreement with what happens in real situation when comparing to the temperature-imposed boundary conditions.

Some comparisons are interesting, however that it is important to mention the differences taken into consideration such as the material and order level of temperature and heat flux imposed. As a general comprehension, the different behaviors are in accordance with literature, though.

6. CONCLUSION

This work studies the mixed convection heat transfer in a laminar and turbulent regimes inside a volumetric receiver used in concentrating solar power plants using Silicon Carbide in the laminar case and Alumina in the turbulent case. Although this is a subject already developed in some countries such as Spain, Germany, USA, Brazil does not have its plant yet. That is why it is so important to stimulate students and teachers on this field. It is a promising clean energy source that can be successfully implemented in Rankine and Brayton cycles, for instance. Therefore, the main contribution of this work is to learn the physics and a mathematical model that are used in this problem and the basic temperature, velocity, and pressure behaviors of the work fluid. Air is significantly heated as it passes through the porous region. In the exit region, that is the region after the porous matrix, temperature ranges from 621K to 796K for the laminar case with temperature-imposed boundary condition. It is worth seeing that the coldest place in this region is in its lower part. There was about a 273% temperature increase when comparing to the inlet air temperature of 293.15K. For the turbulence case, where heat flux is imposed, the temperature behavior in the porous matrix as well as in the exit domain shows a gradient temperature different from that in the laminar case when temperature is imposed as boundary condition. The case with flux imposed to take into consideration as a means of considering the radiation on the absorber surface in the porous matrix seems to be in more accordance with what happens in a real situation and with literature. In a turbulent case, for Alumina, with the entrance velocity (0.01m/s) and heat flux ($100 W/m^2$), the temperature becomes higher when approaching the core of porous domain. It seems that the thermal behavior for heat flux as boundary condition is in more agreement with what happens in real situation when comparing to the temperature-imposed boundary conditions.

7. REFERENCES

Albanakis, C., Missirlis, D., Michailidis, N., Yakinthos, K., Goulas, A., Omar, H., Tsipas, D., Granier, B., 2009. "Experimental analysis of the pressure drop and heat transfer through metal foams used as volumetric receivers under concentrated solar radiation". Experimental Thermal and Fluid Science, Vol. 33, pp. 246–252.

Ávila-Marín, A. L., 2011. "Volumetric receivers in Solar Thermal Power Plants with Central Receiver System technology: A review". Solar Energy, Vol. 85, pp. 891–910.

Behar, O.; Khellaf, A.; Mohammedi, K., 2013. "A Review of studies on central receiver solar thermal power Plants". Renewable and Sustainable Energy Reviews, Vol. 23, pp. 12–39.

Buck, R., Bra¨uning, T., Denk, T., Pfa¨nder, M., Schwarzbo¨zl, P., Tellez, F., 2002. Solar-Hybrid Gas Turbine-based Power Tower Systems (REFOS). In Proceedings of the ASME 201 at Forum 2001, Solar Energy: The Power to Choose, April 21–25, 2001, Washington, DC.

Del Río, A., Korzynietzb, R., Briosoa, JA., Gallasa, M.,. Ordóñeza, I., Queroa, M., and Díaza, C. "Soltrec - Pressurized volumetric solar air receiver technology"

Dowling, A.W., Zheng, T., Zavala, V.M., Economic assessment of concentrated solar power technologies: a review, Renewable Sustainable Energy Rev. 72 (2017) 1019–1032, https://doi.org/10.1016/j.rser.2017.01.006.

He, Y.-L., Qiu, Y., Wang, K., Perspective of concentrating solar power, Energy 198 (2020), 117373, https://doi.org/10.1016/j.energy.2020.117373.

Hossain, M., Wilson, M., 2002. "Natural covectionn flow in a fluid-saturated porous medium enclosed by non-isothermal walls with heat generation". Internnational Journal of Thermal Sciences, Vol. 41, pp. 447-454.

Kribus, A., Grijnevich, M., Gray, Y., Parametric study of volumetric absorber performance, Energy Proc. 49 (2014) 408–417, https://doi.org/10.1016/j.egypro.2014.03.044. A

Kribus, A., Gray, Y., Grijnevich, M., The promise and challenge of solar volumetric absorbers, Sol. Energy 110 (2014) 463–481, https://doi.org/10.1016/j.solener.2014.09.035. B

Li, M.-J., Tao, W.-Q., Review of methodologies and polices for evaluation of energy efficiency in high energy-consuming industry, Appl. Energy 187 (2017) 203–215, https://doi.org/10.1016/j.apenergy.2016.11.039.

Mehos M., Turchi C., Vidal J., Concentrating Solar Power Gen3 Demonstration Roadmap, National Renewable Energy Lab, 2017.

8. RESPONSIBILITY NOTICE

The authors are the only responsible for the printed material included in this paper.

9. ACKNOWLEDGEMENTS

The authors thank **FAPEMIG** (Process: APQ-02457-12) and **LEFTER100** (Laboratory of Computational, Experimental and Numerical Thermal and Fluid Engineering) at UNIFEI, Itabira Campus, Minas Gerais, Brazil.